A molecular analysis of carbon nanotori formation

I-Ling Chang, and Jiu-Wen Chou

Citation: Journal of Applied Physics **112**, 063523 (2012); doi: 10.1063/1.4754538
View online: https://doi.org/10.1063/1.4754538
View Table of Contents: http://aip.scitation.org/toc/jap/112/6
Published by the American Institute of Physics

A molecular analysis of carbon nanotori formation

I-Ling Chang[a] and Jiu-Wen Chou
Department of Mechanical Engineering, National Cheng Kung University, Tainan, Taiwan

(Received 29 March 2012; accepted 24 August 2012; published online 26 September 2012)

This study uses molecular dynamics simulation to examine the geometric criteria and stability of forming a perfect carbon nanotorus without pentagon-heptagon defects or surface buckles. Various nanotube diameters and nanoring diameters of both armchair and zigzag nanotori were relaxed at room temperature, and the equilibrated atomic configurations were inspected. This study uses the coordinate parameter, which illustrates the atomic arrangement around each atom, as an indicator of buckles to avoid misjudgment caused by transient or thermal disturbance. For each nanotube diameter, there exists a critical nanoring diameter beyond which the perfect carbon nanotori can form. This study examines the binding potential energy and deformation energy of the relaxed nanotorus model, showing that the critical nanoring diameter cannot be easily predicted through critical energy consideration because buckling is a form of structural instability. Results show that the structural stability of a perfect nanoring primarily depends on the nanotube diameter and nanoring diameter, whereas its chirality has little effect, and one empirical relation is fitted to determine the critical nanoring diameters. © *2012 American Institute of Physics*.
[http://dx.doi.org/10.1063/1.4754538]

I. INTRODUCTION

Among the various nanomaterials currently available, carbon-based nanostructures exhibit amazingly diverse properties. Since the discovery of carbon nanotubes (CNTs) in the early 1990s, CNTs have attracted a lot of research attention because of their unique structural, physical, and mechanical properties. Fullerene crop circles, referred to as carbon nanorings or nanotori hereafter, commonly appear as side-products in the laser- or deposition-grown process of CNTs.[1–4] Carbon nanotorus structures have generated great interest for their potential novel device applications, as they not only inherit the conductivity of certain carbon nanotubes,[5–8] but also display desirable field-emission behaviors[3] which electrons could be induced under external electromagnetic field. A carbon nanotorus can function as a prototype for studying unusual electronic, magnetic, and even superconductivity properties in a ring-type quantum wire with a turning of the current that creates a magnetic moment.[9] However, the formation and structure of carbon nanotori remain unclear. Two atomic structures of nanotori are typical postulated: one with only a hexagonal carbon-ring formation, and the other containing pentagon-heptagon defects. The physical properties of CNTs, including their conductance, can be significantly influenced by the occurrence of buckling[10] or topological pentagon-heptagon defects. To improve the electronic performance of nanorings, it is highly desirable to reduce the diameter and the number of pentagons-heptagons defects they contain. Hence, this study focuses on the geometry criteria and stability of forming carbon nanotori with only hexagonal carbon-rings.

The formation and growth of carbon nanorings have been the subject of extensive research. Liu *et al.*[1] observed circular formations in single-wall carbon nanotube (SWCNT) ropes while examining laser-grown SWCNT materials using scanning force and transmission electron microscopy. They stated that many of the individual tubes in these circular ropes are perfect tori, with diameters typically ranging between 300 and 500 nm and a rope width of 5-15 nm. Ahlskog *et al.*[2] observed carbon nanorings with scanning electron microscope and atomic force microscope imaging of nanotube deposits produced catalytically by the thermal decomposition of hydrocarbon gas, showing that the rings typically have a diameter of a few hundred nanometers. Martel *et al.*[11] fabricated carbon rings from the folding of straight single-wall carbon nanotubes under ultrasonic irradiation, with yields exceeding 50%. They also discussed the thermodynamic stability of the rings using a simple continuum elastic model, and measure the electrical conductance of the rings as a function of temperature in the presence of a perpendicular magnetic field. Song *et al.*[3,4] proposed a new process for the large-scale growth of single-walled carbon nanorings in high yields by thermally decomposing C_2H_2 in a floating iron catalyst system. They also measured electrical properties of the rings using the Raman spectra. They observed that carbon nanorings, both perfect and open, exhibit field emission behaviors beyond a certain critical voltage. Liu and Stamm[12] achieved ultrahigh-density carbon nanotori arrays, as small as 25 nm, on a silicon wafer using a novel templated solution deposition method that allows for the integration of the rings with silicon and microelectromechanical systems technology. Shea *et al.*[13] reported the magnetoresistance (MR) measurement of single-wall carbon nanotube rings at low temperatures and observed the negative MR characteristic of weak one-dimensional localization from 3 K to 60 K. This resulted from the constructive interference between conjugate electron waves counterpropagating around self-intersecting electron trajectories inside the

[a]Electronic mail: ilchang@mail.ncku.edu.tw.

material, especially with the closed ring geometry providing an additional path for interference.

Atomistic simulations provide an alternative means for analyzing the properties of nanomaterials. Molecular dynamics (MD) simulations are increasingly being used to study the mechanical behavior of nanostructures. Many researchers have investigated the formation of the stable topography of carbon nanorings. One method is to geometrically bend a defect free single-walled straight CNT into a circular ring by connecting its two ends. This approach constructs the nanoring without the involving of defects such as pentagons or heptagons.[14–17] Han[16] investigated the energetics and structures of circular and polygonal single wall carbon nanorings using large-scale molecular simulations and concluded that circular rings with no topological defects are more energetically stable and kinetically accessible than polygonal rings containing pentagon-heptagon defects for the laser-grown SWCNTs and fullerene crop circles. Conversely, Avron and Berger[18] proposed a tiling rule for creating carbon nanorings that corresponds to the toroidal arrangement of trivalent atoms with pentagonal, hexagonal, and heptagonal rings. They concluded that the proposed toroidal carbon nanorings could exist from finding the local minimum of the molecular energy. Itoh and Ihara[19,20] suggested several ways to construct carbon nanorings from graphite carbons C_{240} and C_{250} consisting of pairs of pentagons and heptagons among the hexagons of carbon atoms. Meunier *et al.*[21] examined the stability of large carbon tori using the elasticity theory. They produced tori with a diameter exceeding 200 nm by bending a single-wall nanotube and connecting the two ends together, proving that the resulting structure is stable. Although many studies have already discussed various aspects of the growth and stability condition of carbon nanorings, it is not clear which atomic structures really exist: perfect nanorings with only hexagonal carbon rings, or rings containing pentagon-heptagon defects. Nanorings with a pure hexagon carbon-ring structure are more energetically favorable when the nanoring diameter is large, whereas nanorings with a mixture of hexagons and pentagon-heptagon defects are more energetically favorable when the nanoring diameter is small.[16,21]

This study discusses the geometry criteria and stability of forming a perfect carbon nanotorus without buckles and pentagons or heptagons defects. Using MD simulations based on the Tersoff many-body potential function,[22–24] this study performs a systematic and comprehensive investigation of the energy required to bend a carbon nanotube into a defect-free nanoring. Various nanoring diameters and nanotube diameter with both armchair and zigzag chiralities are simulated to examine the stability of carbon nanorings. This study also investigates the applicability of the elastic beam theory to calculate the deformation energy of bending a straight CNT into a nanoring.

II. SIMULATION METHOD

Straight CNTs can be considered as a graphene sheet rolled into a cylindrical shell, and three distinct types of nanotubes can be classified according to the direction of rolling up: armchair, zigzag, and chiral. To examine the formation and stability of the nanoring, an atomic model with nanoring diameter, D, and nanotube diameter, $2R$, was constructed from bending and connecting two ends of the single-walled straight CNT (Fig. 1). The axial length of the straight CNT must be chosen so that atoms on two ends preserve the complete six-membered carbon-ring structure while connecting. All simulations were performed at room temperature (300 K) using a rescaling method, and Newton's equations of motion were solved using a fifth order Gear's predictor-corrector algorithm. The empirical Tersoff many-body potential,[22–24] which is commonly adopted in CNTs molecular simulation studies to provide quick estimation and significant insight into the thermo-mechanical behavior, was employed to describe the interatomic interaction between the carbon atoms. The force acting on an individual atom was obtained by summing the forces contributed by the surrounding atoms. The initial atomic models of nanorings were relaxed for 30 000 time steps with a 1 fs step size to ensure the rings reached their equilibrium states. To assess the influence of geometry and chirality on the formation of a perfect nanoring without buckling, models with various nanoring diameters, nanotube diameters, and helical types were simulated and their relaxed atomic configurations were inspected. At equilibrium, the potential energy, U, of the atomic system was recorded, with the binding potential energy density defined as

$$u = \frac{U_{ring}}{N}, \tag{1}$$

where N is the number of atoms in the system. The bonding stabilizes as the binding potential energy density reaches its minimum. Meanwhile, the corresponding straight and infinitely long CNTs are equilibrated as an energy benchmark for comparisons. The deformation energy density of the nanoring is defined as the potential energy density difference at the equilibrium as

$$u_s = \frac{U_{ring} - U_{CNT}}{N}, \tag{2}$$

where U_{ring} and U_{CNT}, respectively, represent the potential energies of the nanoring and straight CNT with the same tube diameter.

III. RESULTS AND ANALYSIS

This study uses molecular dynamics simulations to investigate the geometry criteria of forming a perfect carbon nanotorus without buckles or kinks on the surface. The binding

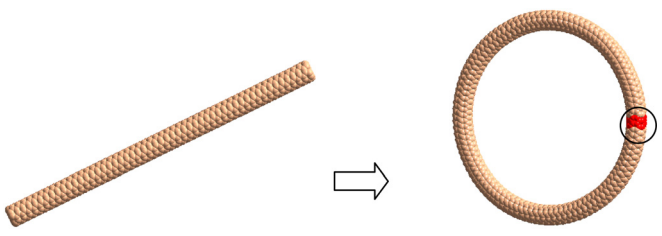

FIG. 1. The schematic presentation of forming the carbon nanotorus model from a straight CNT.

potential energy density and deformation energy density were observed for each equilibrated nanotorus model. First, similar nanotube diameter of (5,5) armchair and (9,0) zigzag carbon nanorings was simulated with various nanoring diameters (2.1-28.2 nm), and Figs. 2 and 3 show the relaxed atomic configurations, respectively. Depending on the nanoring diameter, some nanorings retain a circular shape while others develop ripples at the inner side of the nanoring (Fig. 4). These ripples are unstable transient structures that eventually produce buckles or kinks. There is also a critical nanoring diameter beyond which the nanotori are perfect, without buckling or surface kinks. This threshold is 10.02 nm for (5,5) nanorings and 11.93 nm for (9,0) rings. As the ring diameter decreases, the nanoring becomes susceptible to buckling and kinks appear on the ring surfaces irrespective of the chirality. If the nanoring diameter is too small, some pentagon-heptagon defects other than purely hexagonal carbon-ring structure appear, as clearly illustrated in the radial distribution function in Fig. 5. These defects in the atomic configuration appear to accommodate sharp variations in surface curvature.

Figure 6 shows the binding potential energy densities for various (5,5) and (9,0) nanotori diameters and their corresponding straight CNTs. As the ring diameter increases, the binding potential energy density decreases, approaching that a straight and infinitely long CNT: −7.208 eV/atom for the (5,5) nanotube and −7.216 eV/atom for the (9,0) nanotube. This indicates a decrease in the stored deformation energy density for nanorings with larger ring diameters, which in turn implies the work required for each atom to bend the straight CNT into nanotori is smaller.

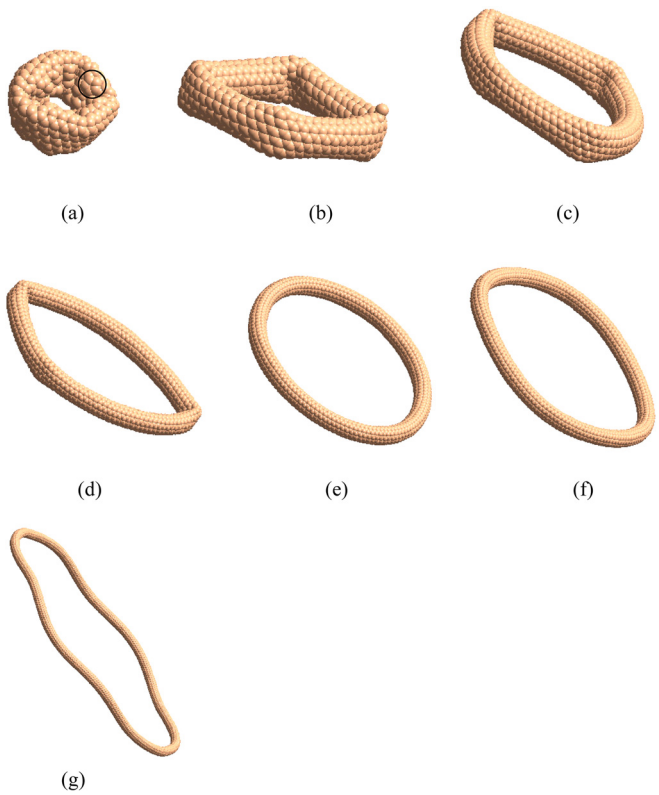

FIG. 2. The relaxed atomic configuration of (5,5) nanorings with different ring diameters, *D*. (a) 2.19 nm (the circle indicate the pentagon defect), (b) 4.07 nm, (c) 5.95 nm, (d) 8.14 nm, (e) 10.02 nm, (f) 11.90 nm, and (g) 28.18 nm.

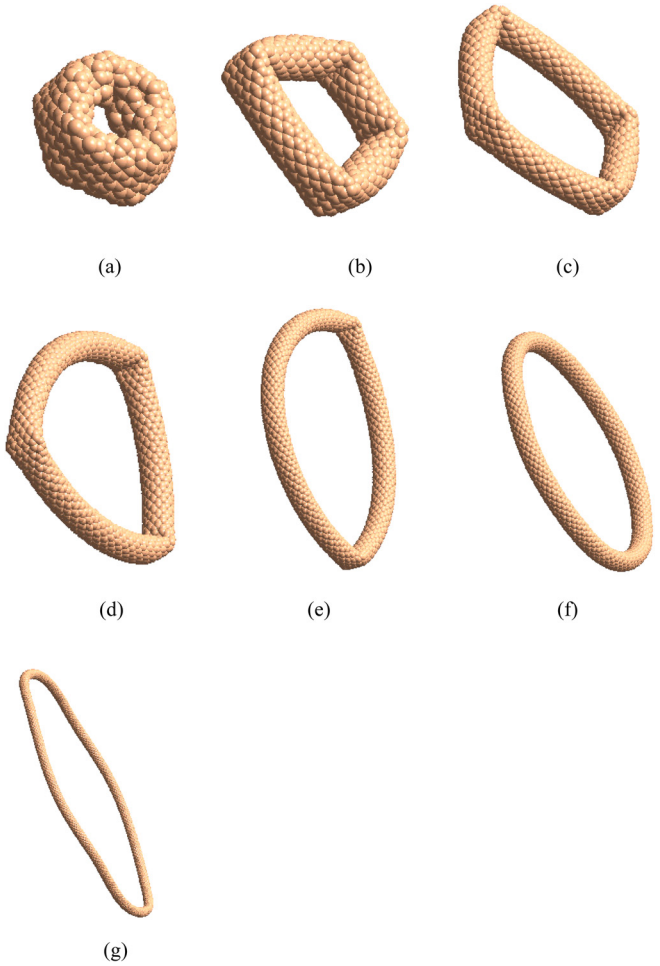

FIG. 3. The relaxed atomic configuration (9.0) nanorings with different nanoring diameters, *D*. (a) 2.17 nm, (b) 3.80 nm, (c) 5.97 nm, (d) 8.14 nm, (e) 10.31 nm, (f)11.93 nm, and (g) 28.20 nm.

This study systematically examines the effects of nanotube diameter and chirality on the critical nanoring diameter of forming a perfect carbon nanotorus. Various tube diameters of armchair, (4,4), (5,5), (6,6), (8,8), (9,9), and zigzag, (7,0), (9,0), (11,0), (13,0), (15,0), carbon nanorings with various ring diameters were relaxed and the atomic configurations at equilibrium were studied. Figure 7 shows the binding potential energy densities for various nanotube diameters

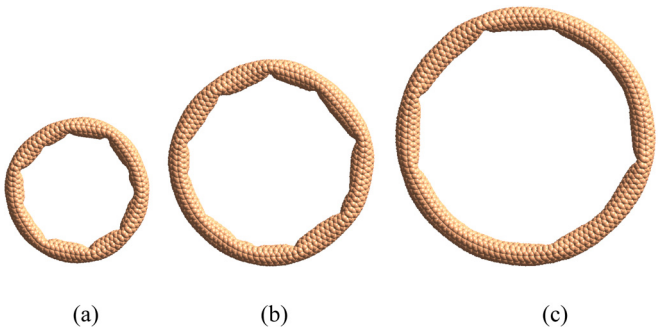

FIG. 4. The unstable configuration of (5,5) nanoring with diameters of (a) 5.95 nm, (b) 8.14 nm, and (c) 10.02 nm.

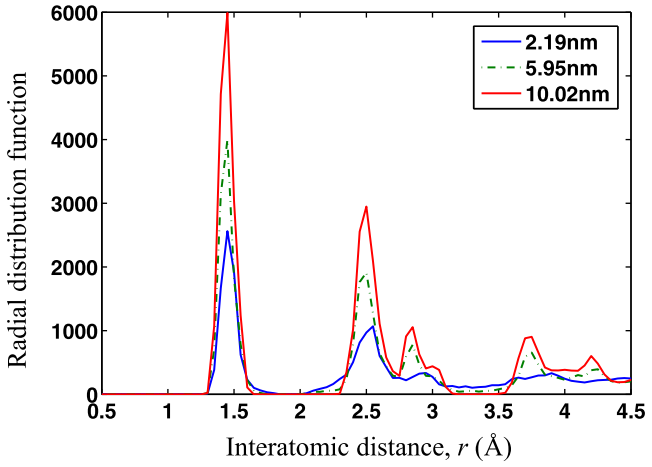

FIG. 5. Radial distribution function for various nanoring diameters of (5,5) nanotori.

and nanoring diameters of armchair and zigzag nanorings. In this figure, solid symbols indicate the critical nanoring diameters beyond which the perfect carbon nanotori can form. The critical binding potential energy densities for perfect

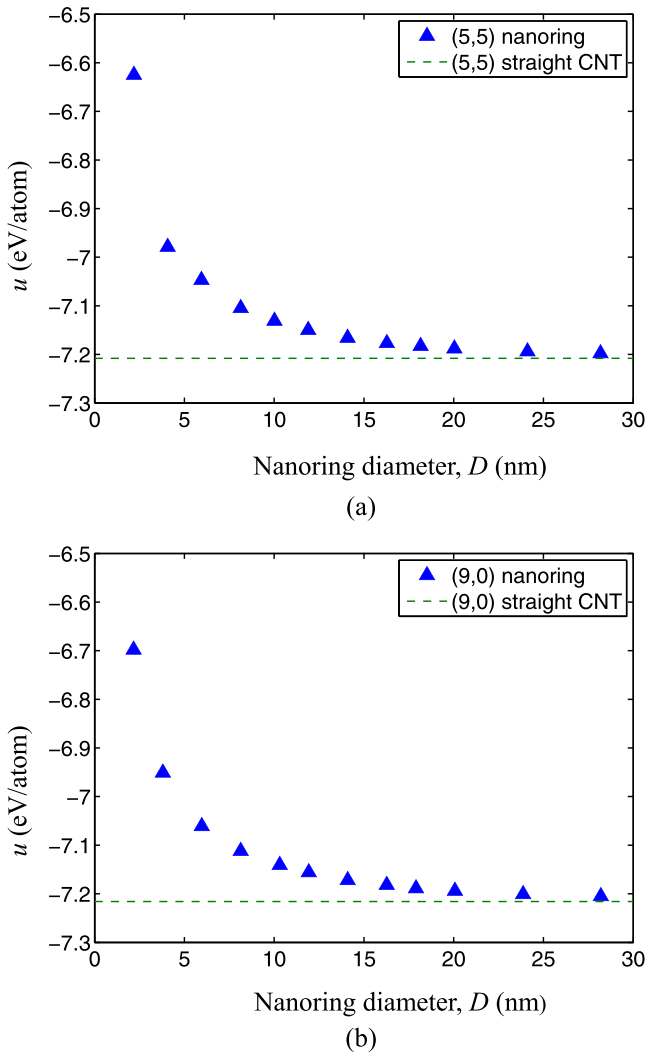

FIG. 6. The binding potential energy densities for (a) (5,5) armchair and (b) (9,0) zigzag carbon nanotori with various nanoring diameters.

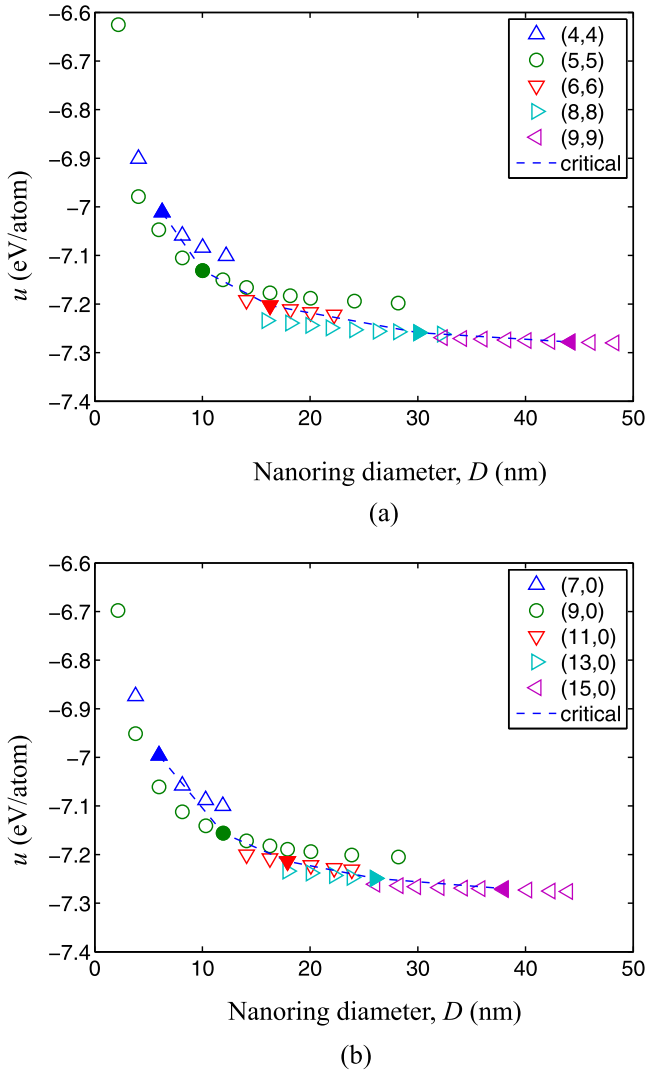

FIG. 7. The binding potential energy densities for (a) armchair and (b) zigzag carbon nanotori with various nanoring diameters and nanotube diameters.

nanorings vary depending on the nanotube diameter. The potential energy per atom is insufficient to identify the energetic stability of perfect nanoring structures with various nanotube sizes. A larger nanotube diameter leads to a lower critical binding potential energy density. The critical ring diameter greatly depends on the nanotube diameter. As the tube diameters become larger, the required critical ring diameter increases accordingly in both armchair and zigzag nanorings. However, it is sometimes difficult to identify whether buckles appear on the surface, especially in large nanotube diameter models. Thus, this study proposes a coordinate parameter, η, as

$$\eta_i = \left| \sum_j \bar{r}_{ij} \right|^2 \tag{3}$$

to facilitate the identification of buckles. For every atom i, the position vectors of atom j within the effective radius of atom i, which is chosen slightly larger than the distance of the second-nearest atom, can be summed up using Eq. (3).

The value of the coordinate parameter shows the neighboring atomic arrangement around each atom and avoids the misjudgment of buckles from transient or thermal disturbance. Figure 8 shows the coordinate parameter plot of the equilibrated (9,9) nanorings with different ring diameters. The surface buckles or kinks are not be easily recognized by visual inspection of the atomic configuration. However, with the assistance of coordinate parameter, it can be seen that the coordinate parameters of atoms around the buckles have much higher value than those at the intact region.

Based on these simulation results, Fig. 9 presents a morphological phase diagram of nanotori with respect to nanotube/nanoring diameters, summarizing the geometric criteria of forming perfect armchair and zigzag nanotori. In this figure, solid symbols indicate perfect carbon nanotori while empty symbols stand for nanotori with surface defects. It is clear to see the boundary between defect-free and buckled nanotori structures. The critical ring diameter increases quadratically, not linearly, as the tube diameter increases. Hence, a quadratic curve function can be fitted to the simulated critical ring diameters as follows:

$$D_c = 0.502(2R)^2 - 3.541(2R) + 10.937. \tag{4}$$

This empirical equation can be used to predict the formation of perfect nanotori in the simulation range. However, the applicability of this empirical relation beyond the simulation geometry remains to be verified.

IV. DISCUSSION

From an energy balance perspective, the work required to bend a straight CNT into a nanoring is stored as the deformation energy in the atomic system. According to elastic theory, it is easy to calculate the deformation strain energy required to elastically bend a hollow cylindrical beam with thickness t and radius R into a ring of diameter D (Fig. 10) as follows:

$$U_s = \pi D \int_0^{2\pi} \int_{R-\frac{t}{2}}^{R+\frac{t}{2}} \frac{2Er^2 \sin^2\theta}{D^2} r dr d\theta = \frac{\pi^2 ERt}{2D}[(2R)^2 + t^2], \tag{5}$$

where E is the Young's modulus of the beam. The larger the ring diameter, the more energetically favorable the defect-free carbon nanoring would be because the deformation energy is smaller. The deformation energy per atom then becomes

$$u_s = \frac{U_s}{N} = \frac{\pi^2 ERt}{2DN}[(2R)^2 + t^2]. \tag{6}$$

Figure 11 shows a comparison of the deformation energy density predicted by elastic beam theory and the simulation results of both (5,5) and (9,0) nanorings. Young's modulus, E, was chosen as 1 TPa[25] and the nanotube diameters of (5,5) and (9,0) nanorings were 6.78 and 7.05 Å. The deformation energy density of both elastic calculation and simulation

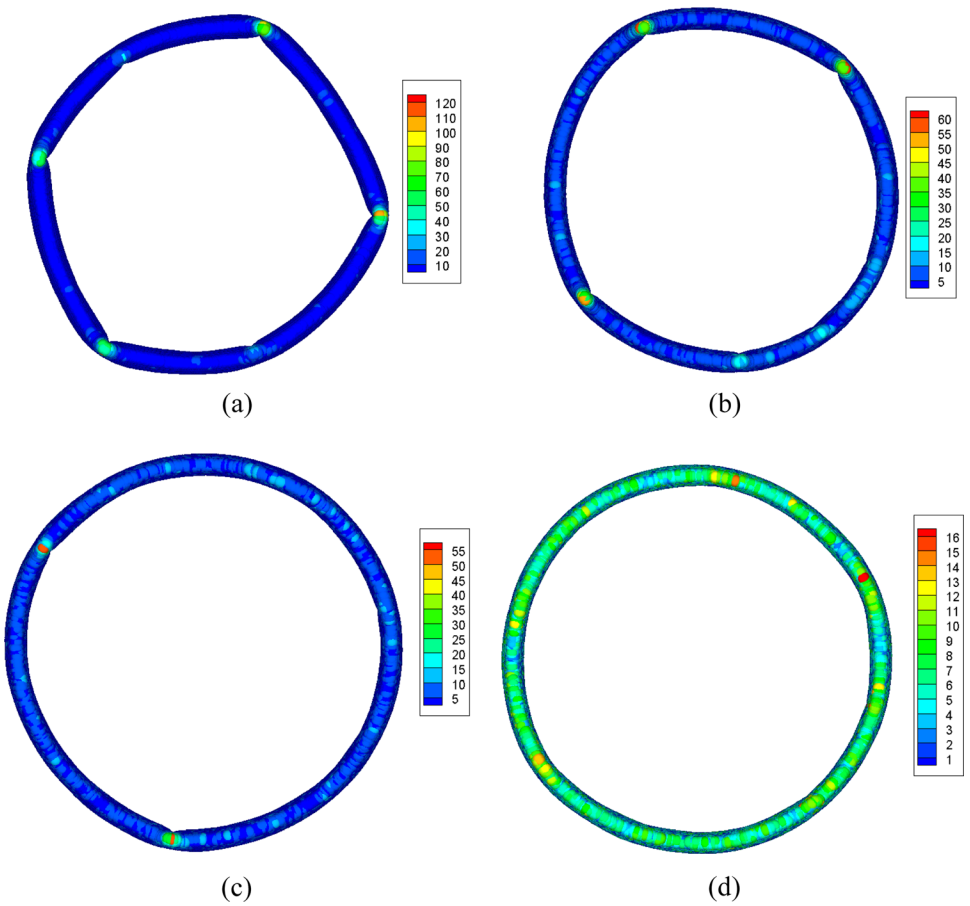

FIG. 8. The coordinate parameter plots for (9,9) nanotori with nanoring diameters of (a) 32 nm, (b) 40 nm, (c) 42 nm, and (d) 44 nm (critical nanoring diameter).

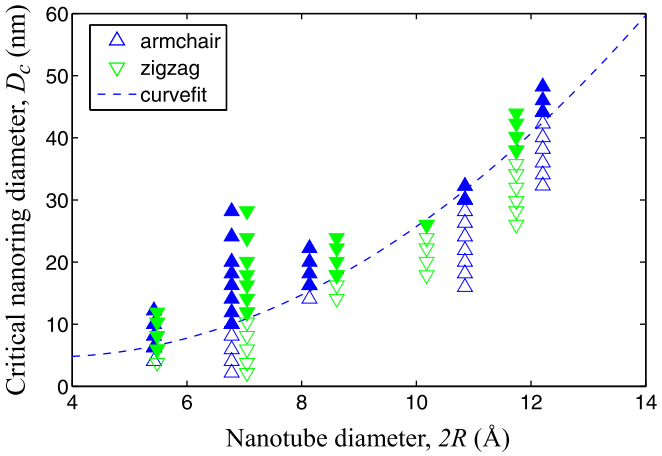

FIG. 9. The morphological phase diagram of nanotori with respect to nanotube/nanoring diameters and the fitting curve of the critical nanoring diameters and nanotube diameters based on simulation data.

results agrees well as long as no buckling appears. This indicates that the elastic beam theory is still applicable for evaluating the deformation energy of perfect nanorings. Once buckles or kinks begin to emerge, the level of deformation energy density decreases which means that the appearance of the buckles decreases the system energy as a mechanism to stabilize the nanoring. The deformation energy required for each atom to turn a straight CNT into a nanoring decreases significantly as the ring diameter increases, indicating that nanorings with a pure hexagon structure are more energetically favorable when the nanoring diameter is large.

In these simulations, the critical diameters for perfect nanorings with only hexagonal carbon-ring formation can be as low as a few tens of nanometers, which are significantly smaller than 200–700 nm observed in experiments.[1–4,11] The reason for this difference is that the lower limit of nanoring diameters is determined in the simulation. Forming the smallest perfect nanoring requires more deformation

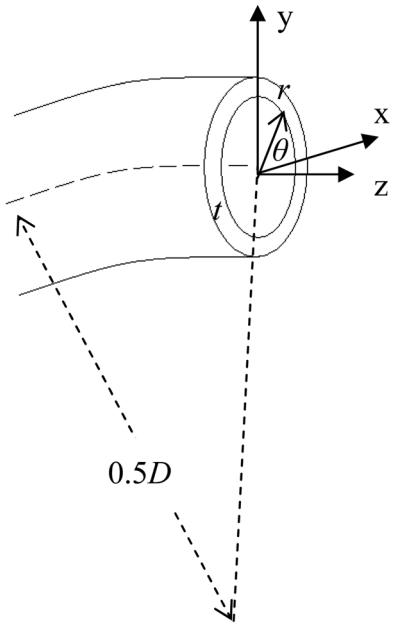

FIG. 10. The schematic presentation of the curved hollow cylindrical beam.

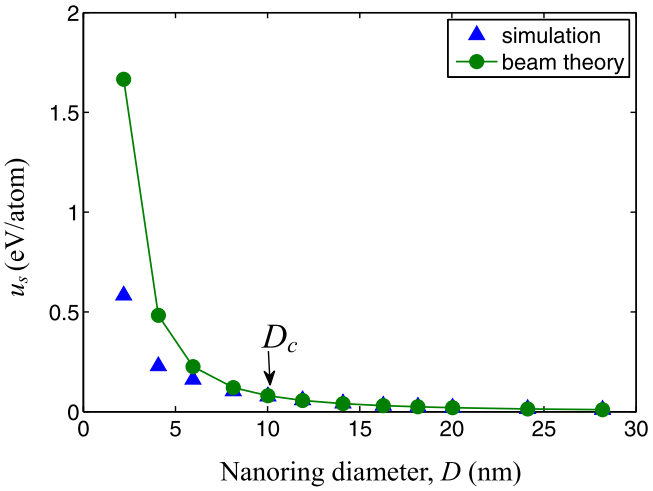

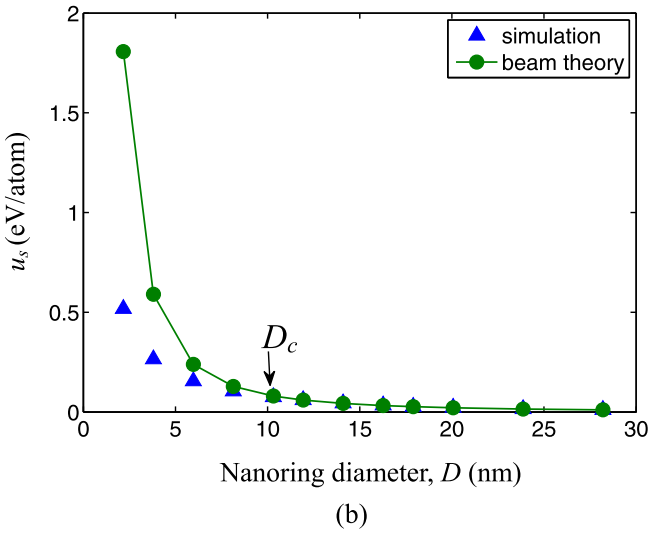

FIG. 11. The comparison of the deformation energy density predicted by elastic beam theory and the simulation results of both (a) (5,5) and (b) (9,0) nanorings.

energy than nanorings with larger diameters. However, these experiments were performed at near-equilibrium conditions under which the energy barrier needed to create the smallest perfect nanoring cannot be overcome.

Meunier *et al.*[21] suggested that the stability of an elastic torus with curvature diameter, D, implies that the C-C bonds are strong enough to accommodate the deformation strain energy. They estimated the critical nanoring diameter based on the bond-breaking energy, $U_b = 4\pi\sigma Rt$, as

$$D_c = \frac{\pi E}{8\sigma}[(2R)^2 + t^2], \tag{7}$$

where σ is the surface tension of graphite perpendicular to the basal planes (4.2 J/m^2)[26] and the wall thickness, t, is chosen as 3.4 Å.[25] Under the assumption that the thickness t remains much smaller than the nanotube radius R, Eq. (7) can be simplified as

$$D_c = \frac{\pi R^2 E}{2\sigma}. \tag{8}$$

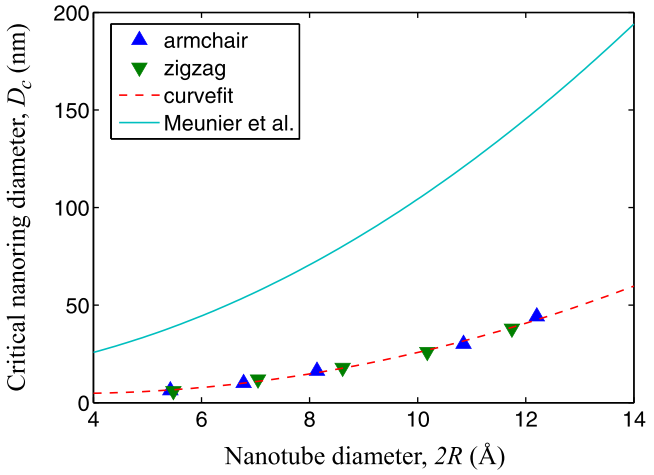

FIG. 12. The comparison between the simulation results and the prediction of the critical nanoring diameters for various nanotube diameters.

Figure 12 shows the estimated critical nanoring diameter by Meunier *et al*. It is interesting to find that the estimated critical ring diameter is much larger than the simulated values even though the trend is consistent. A higher estimated critical ring diameter implies that the required deformation energy is lower for bond breaking than local buckling, which seems counter-intuitive. This contradiction may be the result of underestimating the bond-breaking energy. The buckling behavior is a form of structural instability that cannot be predicted through critical energy consideration.

V. CONCLUSIONS

This study uses molecular dynamics simulations to investigate the geometric criteria of forming a perfect carbon nanotorus without buckles or kinks on the surface. The atomic models of nanotori were constructed by connecting both ends of straight CNTs and then equilibrated at room temperature. Depending on the geometry sizes, some nanorings retained a circular shape whereas others developed ripples at the inner side of the nanoring. These ripples eventually result in buckles or kinks. This study systematically examines the geometry (i.e., nanoring diameter and tube diameter) and chirality effects on forming a perfect carbon nanotorus.

Simulation results indicate that for each nanotube diameter, there exists a critical ring diameter beyond which the nanoring has a purely hexagonal carbon-ring formation and a smooth nanoring surface without buckling. If the nanoring diameter is too small, some pentagon-heptagon defects, other than purely hexagonal structure, appear in the atomic configuration to accommodate sharp variations in surface curvature. The critical nanoring diameter increases as the nanotube diameter increases, revealing one empirical relationship for predicting the critical nanoring diameter. The deformation energy density of bending a hollow cylindrical beam into a circular ring was calculated based on elastic beam theory. The deformation energy density of both elastic calculation and simulation results agreed quite well as long as no buckling appeared, indicating that the elastic beam theory is still applicable to evaluating the deformation energy of perfect nanorings. Once the buckles or kinks begin to emerge, the level of deformation energy density decreases, which means that the appearance of the buckles lowers the system energy as a mechanism to stabilize the nanoring. The estimated critical nanoring diameter by Meunier *et al*. was much larger than the simulation results although the trend was consistent.

ACKNOWLEDGMENTS

This study is supported by the National Science Council of Taiwan under Grant Nos. NSC 98-2221-E-194-012-MY2 and NSC 99-2923-E-006-006-MY3. The authors are also grateful to the Taiwan National Center of High-Performance Computing for providing computer time and facilities.

[1]J. Liu, H. Dai, J. H. Hafner, D. T. Colbert, R. E. Smalley, S. J. Tans, and C. Dekker, Nature **385**, 780 (1997).
[2]M. Ahlskog, E. Seynaeve, R. J. M. Vullers, C. Van Haesendonck, A. Fonseca, K. Hernadi, and J. B. Nagy, Chem. Phys. Lett. **300**, 202 (1999).
[3]L. Song, L. Ci, C. Jin, P. Tan, L. Sun, W. Ma, L. Liu, D. Liu, Z. Zhang, Y. Xiang, S. Luo, X. Zhao, J. Shen, J. Zhou, W. Zhou, and S. Xie, Nanotechnology **17**, 2355 (2006).
[4]L. Song, L. Ci, L. Sun, C. Jin, L. Liu, W. Ma, D. Liu, X. Zhao, S. Luo, Z. Zhang, Y. Xiang, J. Zhou, W. Zhou, Y. Ding, Z. Wang, and S. Xie, Adv. Mater. **18**, 1817 (2006).
[5]A. Thess, R. Lee, P. Nikolaev, H. Dai, P. Petit, J. Robert, C. Xu, Y. H. Lee, S. G. Kim, D. T. Colbert, G. Scuseria, D. Tomanek, J. E. Fischer, and R. E. Smalley, Science **273**, 483 (1996).
[6]H. Dai, A. Rinzler, P. Nikolaev, A. Thess, D. T. Colbert, and R. E. Smalley, Chem. Phys. Lett. **260**, 471 (1996).
[7]S. J. Tans, M. H. Devoret, H. Dai, A. Thess, R. E. Smalley, L. J. Geerlings, and C. Dekker, Nature **386**, 474 (1997).
[8]J. E. Fischer, H. Dai, A. Thess, R. Lee, N. M. Hanjani, D. DeHaas, and R. E. Smalley, Phys. Rev. B **55**, R4921 (1997).
[9]R. C. Haddon, Nature **388**, 31 (1997).
[10]A. A. Farajian, B. I. Yakobson, H. Mizuseki, and Y. Kawazoe, Phys. Rev. B **67**, 205423 (2003).
[11]R. Martel, H. R. Shea, and P. Avouris, J. Phys. Chem. B **103**, 7551 (1999).
[12]X. Liu and M. Stamm, Macromol. Rapid Commun. **30**, 1345 (2009).
[13]H. R. Shea, R. Martel, and P. Avouris, Phys. Rev. Lett. **84**, 4441 (2000).
[14]M. Huhtala, A. Kuronen, and K. Kaski, Comput. Phys. Commun. **146**, 30 (2002).
[15]M. Huhtala, A. Kuronen, and K. Kaski, Comput. Phys. Commun. **147**, 91 (2002).
[16]J. Han, Chem. Phys. Lett. **282**, 187 (1998).
[17]L. Liu, C. S. Jayanthi, and S. Y. Wu, Phys. Rev. B **64**, 033412 (2001).
[18]J. E. Avron and J. Berger, Phys. Rev. A **51**, 1146 (1995).
[19]S. Itoh and S. Ihara, Phys. Rev. B **48**, 8323 (1993).
[20]S. Itoh and S. Ihara, Phys. Rev. B **49**, 13970 (1994).
[21]V. Meunier, P. Lambin, and A. A. Lucas, Phys. Rev. B **57**, 14886 (1998).
[22]J. Tersoff, Phys. Rev. Lett. **56**, 632 (1986).
[23]J. Tersoff, Phys. Rev. B **37**, 6991 (1988).
[24]J. Tersoff, Phys. Rev. B **39**, 5566 (1989).
[25]J. P. Lu, Phys. Rev. Lett. **79**, 1297 (1997).
[26]M. S. Dresselhaus, G. Dresselhaus, K. Sugihara, I. L. Spain, and H. A. Goldberg, *Graphite Fibers and Filaments* (Springer, Berlin, 1988).